Available online at www.sciencedirect.com

SciVerse ScienceDirect

Ceramics International 39 (2013) 2185–2195

CERAMICS INTERNATIONAL

www.elsevier.com/locate/ceramint

Review paper

Piezoresponse force microscopy characterization of rare-earth doped $BiFeO_3$ thin films grown by the soft chemical method

C.R. Foschini[a], M.A. Ramirez[b], S.R. Simões[b], J.A. Varela[a], E. Longo[a], A.Z. Simões[b,*]

[a]*Laboratório Interdisciplinar em Cerâmica (LIEC), Departamento de Físico-Química, Instituto de Química, Unesp, CEP: 14800-900, Araraquara, SP, Brazil*

[b]*Universidade Estadual Paulista—Unesp—Faculdade de Engenharia de Guaratinguetá, Av. Dr. Ariberto Pereira da Cunha, 333, Bairro Pedregulho, CEP 12516-410, Guaratinguetá, SP, Brazil*

Received 6 July 2012; received in revised form 27 August 2012; accepted 27 August 2012
Available online 4 September 2012

Abstract

The multiferroic behavior with ion modification using rare-earth cations on crystal structures, along with the insulating properties of $BiFeO_3$ (BFO) thin films was investigated using piezoresponse force microscopy. Rare-earth-substituted BFO films with chemical compositions of $(Bi_{1.00-x}RE_xFe_{1.00}O_3$ ($x=0$; 0.15), RE = La and Nd were fabricated on Pt (111)/Ti/SiO_2/Si substrates using a chemical solution deposition technique. A crystalline phase of tetragonal BFO was obtained by heat treatment in ambient atmosphere at 500 °C for 2 h. Ion modification using La^{3+} and Nd^{3+} cations lowered the leakage current density of the BFO films at room temperature from approximately 10^{-6} down to 10^{-8} A/cm^2. The observed improved magnetism of the Nd^{3+} substituted BFO thin films can be related to the plate-like morphology in a nanometer scale. We observed that various types of domain behavior such as 71° and 180° domain switching, and pinned domain formation occurred. The maximum magnetoelectric coefficient in the longitudinal direction was close to 12 V/cm Oe.

Keywords: A. Films; B. Interfaces; C. Dielectric properties; C. Ferroelectric properties

Contents

1. Introduction . . . 2185
2. Experimental procedure . . . 2186
3. Results and discussion . . . 2187
4. Conclusions . . . 2193
Acknowledgments . . . 2193
References . . . 2193

1. Introduction

The $BiFeO_3$-based multiferroics are interesting materials for basic research as well as for possible application in magnetoelectric devices [1,2]. Antiferromagnetic ordering in $BiFeO_3$ occurs at nearly 620 K [1–3] whereas dipole ordering associated with a first-order rhombohedral–orthorhombic structural transition takes place in the range 1090–1100 K [4–6]. Below room temperature two magnetic transitions at 200 K and 140 K have been revealed [7,8]. Dipole ordering is the result of a stereochemical activity of the $6s^2$ electron pair of Bi^{3+} ion and occurs via the relative shift of Bi^{2+}, Fe^{3+} and O^{2-} ions along [001] hexagonal

*Corresponding author. Tel.: +55 12 3123 2765.
E-mail address: alezipo@yahoo.com (A.Z. Simões).

0272-8842/$ - see front matter © 2012 Elsevier Ltd and Techna Group S.r.l. All rights reserved.
http://dx.doi.org/10.1016/j.ceramint.2012.08.083

axes. Crystal structure of $BiFeO_3$ is described with the space group R3c, allowing a linear magnetoelectric effect. However, in the bulk samples no linear magnetoelectric effect was observed, because the G type antiferromagnetic structure is modulated by cycloid with a period of 620 A [3,9]. $BiFeO_3$ shows metamagnetic transition in magnetic fields above 18 T at 5 K [10]. This transition is associated with a collapse of the incommensurately modulated magnetic structure. As a result of the transition a weak ferromagnetic state appears. In the weak ferromagnetic state a large linear magnetoelectric effect was observed [11]. BFO has a distorted perovskite structure in a rhombohedral system (lattice parameters: $a=3.958$ Å, $\alpha=89.30^\circ$ [1–3]). BFO has a potential to exhibit a large spontaneous polarization (*Ps*) value [6–9]. Although only *Ps* values of approximately 6 μC/cm^2 have been reported for BFO bulk [10] the first-principles study predicted that BFO crystal possesses theoretical *Pr* values of 90–100 μC/cm^2 potentially [11]. Wang et al. reported remanent polarization (*Pr*) values of 50–60 μC/cm^2 for BFO films with a pseudotetragonal system heteroepitaxially grown on (100) $SrRuO_3$/(100) $SrTiO_3$ substrates by pulsed laser deposition (PLD) [12]. Furthermore, Yun et al. also deposited tetragonal BFO films with a giant ferroelectric polarization beyond 150 μC/cm^2 on Pt/TiO_2/SiO_2/Si substrates by PLD [13]. However, BFO bulks and thin films always suffer from low electrical resistivities, preventing these materials from exhibiting essential polarization performance at room temperature [14,15]. For example, appropriate evaluation of *Ps* and *Pr* values has never been achieved on BFO films fabricated by solution deposition techniques due to the high leakage current conduction. Similar phenomena have already been observed in the case of $Bi_4Ti_3O_{12}$ (BIT) films that also have low electrical resistivity [16]. Furthermore, Eerenstein et al. argued that the enhanced polarization of BFO films reported in previous works would be ascribed to extra charge inflow based on the leakage current and that the improvement of the electrical resistivity is essential for evaluating intrinsic polarization property of the BFO film [17]. Béa et al. [18] also explained that conductive path in the BFO film, such as Bi_2O_3, Fe_2O_3, etc., would prevent their practical use as ferroelectric elements.

Recently, researchers have proposed a material-design concept for reducing the electrical conduction of perovskite based ferroelectric thin films. The material-design concept is based on ion substitution to eliminate oxygen vacancies that act as conduction carriers in perovskite-based crystal [16,19,20]. For example, Bi-site substitution using some rare-earth cations, such as La^{3+}; Nd^{3+} and Sm^{3+} effectively enhanced the insulating property of the BIT film, which is ascribed to the compensation of the volatile Bi component in the BIT crystal by the rare-earth cations to suppress the formation of oxygen vacancies [21–24]. The trial to reduce the electrical conduction based on the material-design concept had already succeeded in the case of some Bi-based ferroelectrics such as $SrBi_2Ta_2O_9$ (SBT) and BIT, as well as Pb-based ferroelectrics such as lead titanate $PbTiO_3$ (PT) and lead zirconate titanate $PbZr_{1-x}Ti_xO_3$ (PZT) [25–27]. Some researchers reported that certain rare-earth cations, such as La^{3+}, Nd^{3+}, Gd^{3+} and Dy^{3+}, can be substituted for the Bi^{3+} ion in the BFO crystal [4,28–30]. The present authors also applied the same approach to improving the electrical resistivity of BFO thin film; some of the volatile Bi^{3+} ions in the BFO crystal were replaced by some nonvolatile rare earth ions to prevent the formation of oxygen vacancies that degrade the insulating and ferroelectric properties. In other work, researchers fabricated La^{3+} and Nd^{3+} substituted BFO films using a chemical solution deposition (CSD) technique and then clarified that replacing 5% of the Bi^{3+} in the BFO crystal with La^{3+} or Nd^{3+} could lower the leakage current density at room temperature significantly [31]. These results indicate that the material-design concept mentioned above is effective for reducing the electrical conduction of the BFO film. We investigated the influence of rare-earth cation substitution on the crystal structure and ferroelectric properties, as well as the electrical resistivity, of BFO film. Two rare-earth cations, i.e., La^{3+} and Nd^{3+} were selected as the substituent cations in this study because the radii of these ions (1.032 and 0.98 Å) with six coordination were similar to that of the Bi^{3+} ion (1.030 Å) with six coordination allowing these ions to occupy the Bi site in the BFO crystal [32]. The magnetoelectric (ME) coefficient $\alpha ME = d\tilde{E}dH = d\tilde{V}$ (tdH) is the most critical indicator for the magnetoelectric coupling properties in multiferroic materials, where V is the induced magnetoelectric voltage, H is the exciting ac magnetic field, and t is the thickness of the sample used for measuring V across the laminate [33]. Our group has expanded significant effort in develop synthetic routes of $BiFeO_3$ thin films [34,35] and we have previously reported the preparation of bismuth base compounds thin films grown on Pt(111)/Ti/SiO_2/Si substrates with good structural, microstructural and electrical properties by the soft chemical method [36–41]. In the present investigation and as a natural extension of previous work, the La^{3+} and Nd^{3+} substituted BFO films were fabricated on Pt(111)/Ti/SiO_2/Si substrates by the soft chemical method. Structural and electrical properties of the films, mainly related to piezoresponse behavior were investigated by using various techniques with a view to explore their technological applications with rare-earth substitution.

2. Experimental procedure

Iron (III) nitrate nonahydrate [$Fe(NO_3)_3 \cdot 9H_2O$], 99.5% purity (Merck), bismuth oxide [Bi_2O_3], 99.9% purity (Aldrich), neodymium oxide [Nd_2O_3], 99.5% purity (Merck), lanthanum oxide [La_2O_3], 99.5% purity (Aldrich) were used as raw materials. The precursor solutions of bismuth, lanthanum, neodymium and iron were prepared by adding the raw materials to ethylene glycol and concentrated aqueous citric acid under heating and stirring. Appropriate quantities of solutions of Fe, Nd, La and Bi were mixed and

homogeneized by stirring at 90 °C. The molar ratio of metal:citric acid:ethylene glycol was 1:4:16. The viscosity of the resulting solution was adjusted to 20 cP by controlling the water content using a Brookfield viscosimeter. The films were spin-coated from the deposition solution onto a Pt (111)/Ti/SiO_2/Si substrate. $Bi_{1.00-x}RE_xFe_{1.00}O_3$ ($x=0$ and $x=0.15$) (BFO, BLF and BNF) were annealed at 400 °C for 2 h with heating rate of 3 °C/min in a conventional furnace and later crystallized at 500 °C for 2 h in static air. Multilayered films were obtained by spinning 10 times the deposition solution on the surface of the substrate at 5000 rpm for 30 s. The number of layers was fixed as a function of the desired thickness to obtain good electrical properties. An excess of 5 wt% Bi was added to the solution, aiming to minimize the bismuth loss during the thermal treatment. Without this additional bismuth the pure phase could not be obtained. Phase analysis of the films was performed at room temperature by X-ray diffraction (XRD) patterns recorded on a (Rigaku-DMax 2000PC) with Cu-Kα radiation in the 2θ range from 20° to 80° with 0.3°/min. The thickness of the annealed films was studied using scanning electron microscopy (SEM-Topcom SM-300) by looking at the transversal section. In this case, back-scattered electrons were utilized. Three measurements were done and the average value of thickness was close to 300 nm. Surface roughness (RMS) was examined by AFM, using tapping mode techniques. Next, a 0.5 mm diameter top Au electrode was sputtered through a shadow mask at room temperature. After deposition of the top electrode, the film was subjected to a post-annealing treatment in a tube furnace under oxygen atmosphere at 300 °C for 1 h. Here, the desired effect was to decrease eventually present oxygen vacancies. The *J–V* measurements were recorded on the Radiant technology tester in the current–voltage mode, with a voltage changing from 0 to +10 V, from +10 to −10 V and back to 0 V. Magnetization measurements were taken using a vibrating-sample magnetometer (VSM) from Quantum Design™. The dc magnetic bias field was produced by an electromagnet (Cenco Instruments J type). The time-varying dc field was achieved by a programmable dc power supply (Phillips PM2810 60 V/5 A/60 W). To measure the dc magnetic field, a Hall probe was employed. The magnetoelectric signal was measured by using a lock-in amplifier (EG&G model 5210) with input resistance and capacitance of 100 MΩ and 25 pF, respectively. Piezoelectric measurements were carried out using a setup based on an atomic force microscope in a Multimode Scanning Probe Microscope with Nanoscope IV controller (Veeco FPP-100). In our experiments, piezoresponse images of the films were acquired in ambient air by applying a small ac voltage with amplitude of 2.5 V (peak to peak) and a frequency of 10 kHz while scanning the film surface. To apply the external voltage we used a standard gold coated Si_3N_4 cantilever with a spring constant of 0.09 N/m. The probing tip, with an apex radius of about 20 nm, was in mechanical contact with the uncoated film surface during the measurements. Cantilever vibration was detected using a conventional lock-in technique.

3. Results and discussion

Fig. 1 shows XRD patterns of nonsubstituted ($x=0$), La^{3+} and Nd^{3+} substituted BFO films. All films consisted of the crystalline BFO phase without a preferential orientation. The nonsubstituted BFO film contained a trace amount of Bi_2O_3 and $Bi_2Fe_2O_9$ phases, while it disappeared in the La^{3+} and Nd^{3+}-substituted BFO films. These results suggest that rare-earth-substitution prevents the generation of the secondary phase. Rare-earth substitution did not affect the crystal orientation of the BFO films although the peaks are shifted to low 2θ angles. This suggests that the addition of rare-earth can either eliminate oxygen vacancies or avoid compositional fluctuations of Fe^{3+} to Fe^{2+} oxidation state influencing on the appearance of secondary phases. The polycrystalline nature of the film can be attributed to the differences in nucleation energy between the ferroelectromagnetic material and the metallic electrode. According to the pattern, the film has a tetragonal perovskite structure. Besides BFO peaks, the characteristic peak for (111) platinum coated silicon substrates at $2\theta=40°$ was identified.

Changes on the surface morphology of the La^{3+} and Nd^{3+} substituted BFO films were evaluated by AFM measurements (Fig. 2a–c). Rare-earth addition tends to suppress the grain growth which is consistent with the XRD results where a decrease in peak sharpness and intensity was observed. The decrease of grain size of rare-earth-doped BFO films can be interpreted by the suppression of oxygen vacancy concentration, which results in slower oxygen ion motion and consequently lower grain growth rate. Nonsubstituted BFO thin films exhibited the inhomogeneous microstructures consisting of small and large grains (80–100 nm) with a statistical roughness, root mean square (RMS) of approximately 6.2 nm. La and Nd-substitution was found to be effective

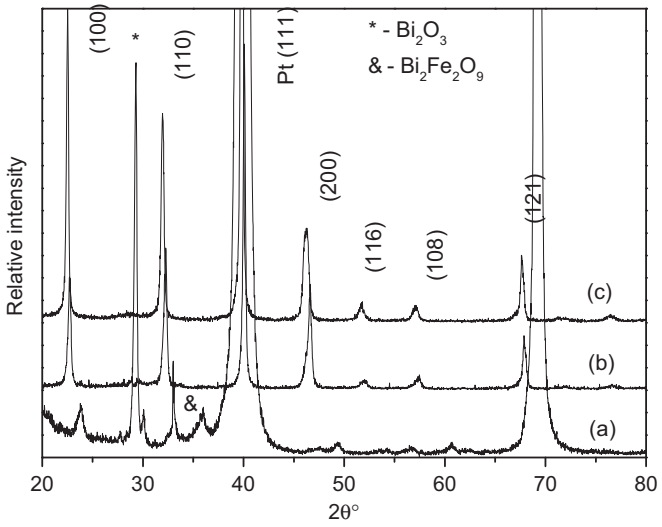

Fig. 1. X-ray diffraction of thin films deposited by the polymeric precursor method at 500 °C in static air for 2 h (a) BFO; (b) BLF and (c) BNF.

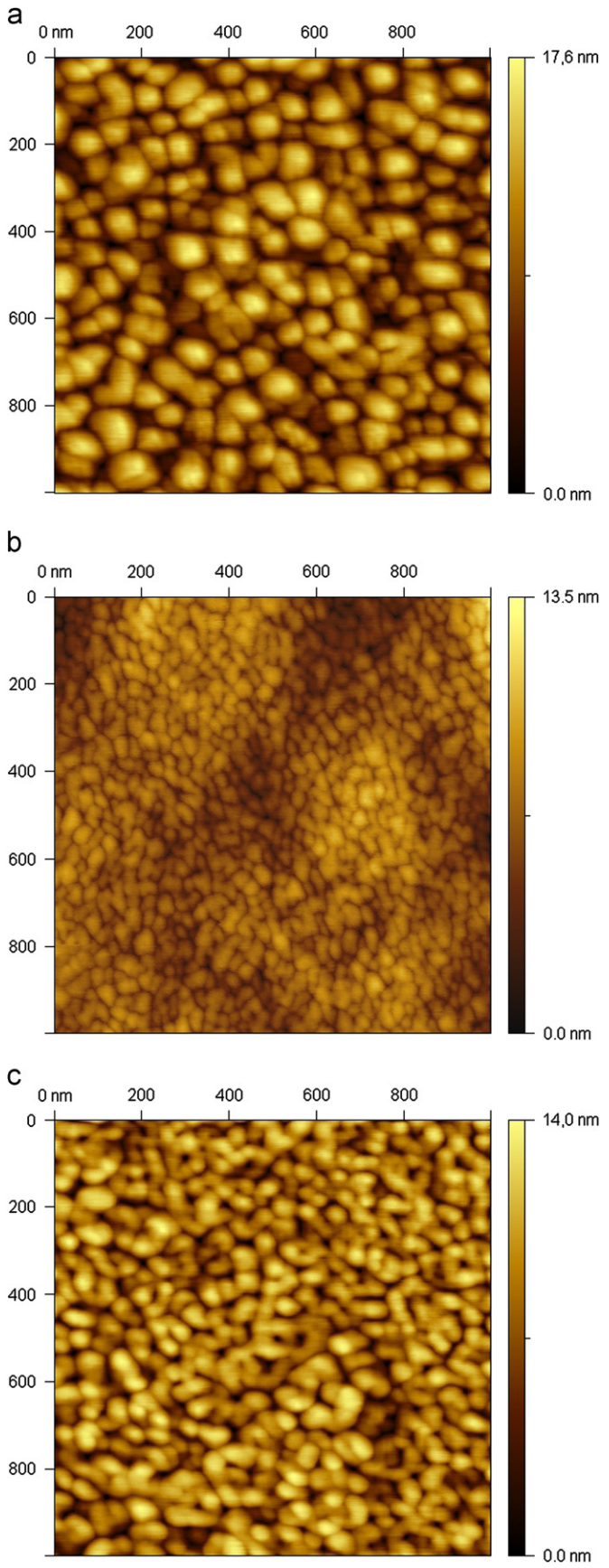

Fig. 2. Atomic force microscopy of thin films deposited by the polymeric precursor method at 500 °C in static air for 2 h (a) BFO; (b) BLF and (c) BNF.

in improving the surface morphology of synthesized BFO-based films, because the precursor film underwent the optimized nucleation and growth process producing films with a homogeneous and dense microstructure. La-substitution reveals rounded grain morphology (60 nm) with [RMS: 5.4 nm] which can be explained by the largest number of tied up hydrogen, which increase the possibility of a homogeneous interaction between any of the carboxyl group (Fig. 2b). Nd-substitution reveals plate-like grains morphology which can be explained by the complexation of the Nd ions by the carboxylic groups (Fig. 2c). The complexation of Bi and Nd by the citric acid leads to a linear polymer and a typical plate-like morphology. In this case there is minor hydrogen number, decreasing the symmetry of the molecule and the possibilities of a homogeneous interaction. The difference in the shape of the grains could be the fact that the complexation of the metals by the carboxilics groups is dependent of the ionic radii of these ions (1.032 and 0.98 Å). The complexation of Bi and Nd by the citric acid leads to a linear polymer and a typical plate-like morphology. Meanwhile, the addition of La competes with the citric acid for the complexation of the bismuth site making the volumetric effect more pronounced and leading to a rounded morphology. Among these films, BNF thin films exhibited the most homogeneous microstructure with [RMS: 4.6 nm] and grain size of 70 nm as shown in Fig. 2(c). Also, the homogeneous microstructure of BNF films may affect the ferroelectric properties, because the voltage can be applied uniformly onto it. The role of rare-earth is to eliminate vacancies which act as point defects and therefore decrease the surface heterogeneity in the films.

An analysis of the evolution of Raman spectra in the rare-earth modified bismuth ferrite shows the order-disorder degree of the atomic structure at short range (Fig. 3). The modes further split into longitudinal and transverse components due the long electrostatic forces associated with lattice ionicity. Substitution of La and Nd in the A-site of the lattice reduces the distortion of octahedral clusters having little influence in the relative intensity of the bands. The vibrational modes located at 224, 355, 385, 531, and 564 cm^{-1} result from the FeO_6 octahedral (Fe=5 or Fe=6). The band located below 200 cm^{-1} is due to the different sites occupied by bismuth within the perovskite layer. Raman frequencies are not strongly affected by rare-earth substitution. Slight changes which occur above 200 cm^{-1} in the BFO can be associated to structural distortion and reduction of vibrations in the FeO_5 octahedra. Rare-earth atoms substitute bismuth within the perovskite structure having marginal influence in the interactions between the $(Bi_2O_2)^{2+}$ layers and perovskite.

Fig. 4 shows the leakage current density (J) vs voltage (V) curves of the rare-earth BFO films measured at room temperature, together with that of the nonsubstituted BFO film. The current density of nonsubstituted BFO film was higher than those of the rare-earth-substituted BFO films

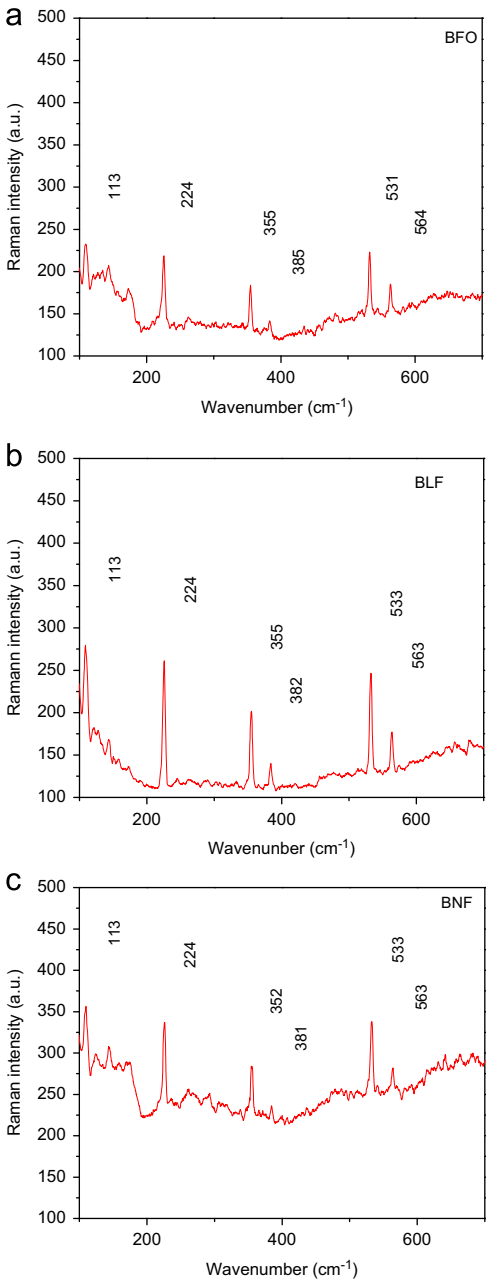

Fig. 3. MicroRaman spectra of thin films deposited by the polymeric precursor method at 500 °C in static air for 2 h (a) BFO; (b) BLF and (c) BNF.

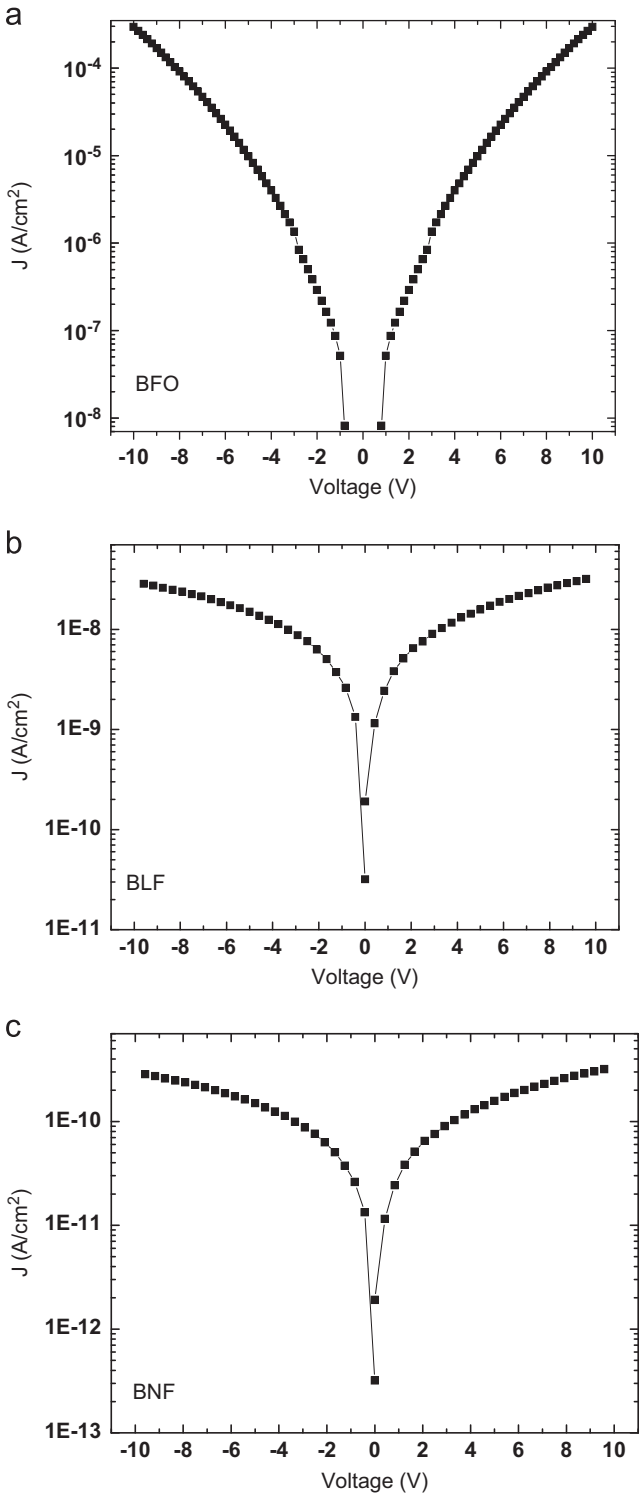

Fig. 4. Leakage current density versus applied electric field of thin films deposited by the polymeric precursor method at 500 °C in static air for 2 h (a) BFO; (b) BLF and (c) BNF.

especially above 4 V. Differences in J–V characteristics were attributed to the suppression of the oxygen vacancies in the BFO films by the rare-earth substitution of the volatile Bi element which is similar to PT, PZT, and BIT films or crystals [42–49]. The leakage current densities of these films were less than 10^{-8} A/cm^2 for the $La^{3+}$and Nd^{3+}-substituted BFO films. On the other hand, the leakage current density of the nonsubstituted BFO film was on the order of 10^{-6} A/cm^2, which was higher than those of the rare earth-substituted BFO films. These results indicate that the nonsubstituted BFO film has a higher leakage current density than La^{3+} and Nd^{3+}-substituted BFO films. These results suggest that the rare-earth-substituted BFO films still contained a certain conducting path, such as a valence change in Fe^{3+} cation [50], whereas the rare-earth substitution lowered the leakage current density by the suppression of oxygen vacancies in the BFO films.

Magnetization (M) versus magnetic field (H) loops were recorded at 300 K (Fig. 5). The nonsubstituted BFO film magnetization was observed with a magnetic field of 1.3 emu/g. A weak ferromagnetic response was noted, although enhanced magnetization was observed as compared to bulk specimens. Gehring [51] and Goodenough and Lango [52] suggested that the statistical distribution of a Fe^{3+} ion in octahedral or the creation of lattice defects might lead to bulk magnetization and weak

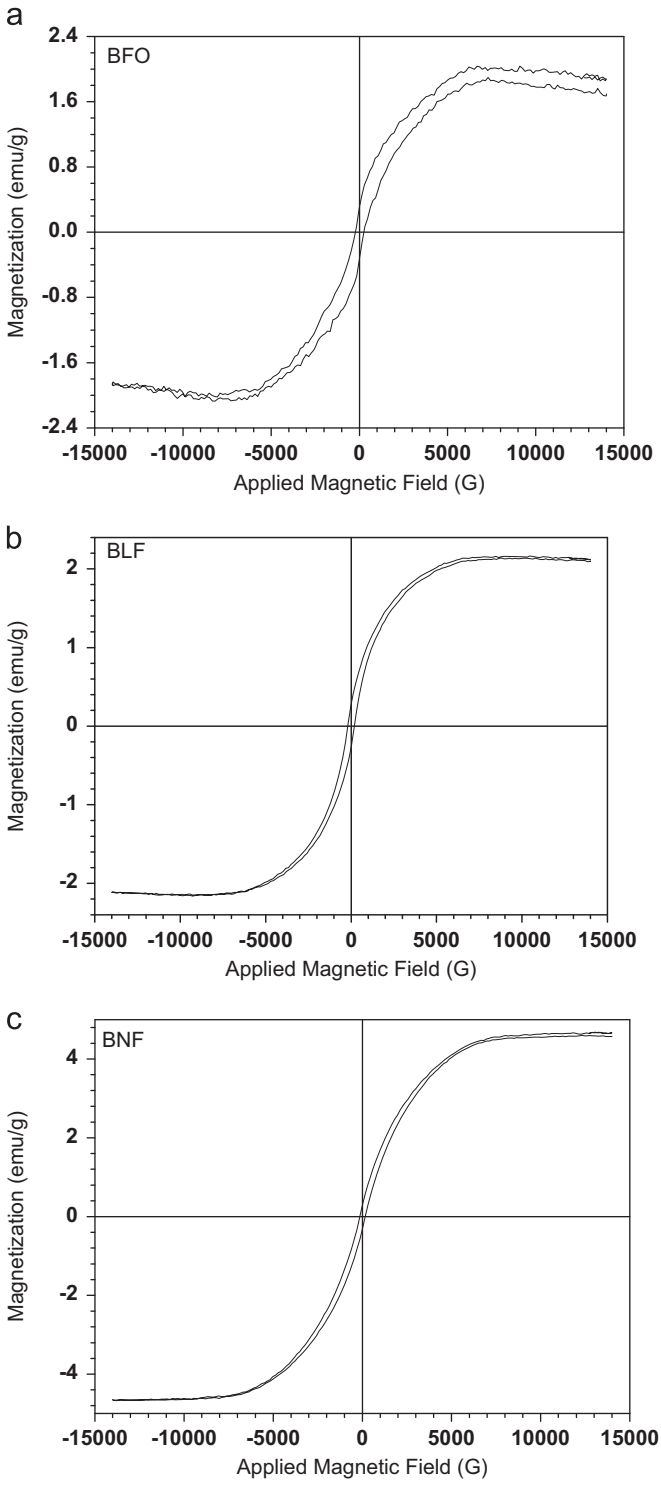

Fig. 5. Field dependencies of the magnetization obtained of thin films deposited by the polymeric precursor method at 500 °C in static air for 2 h (a) BFO; (b) BLF and (c) BNF.

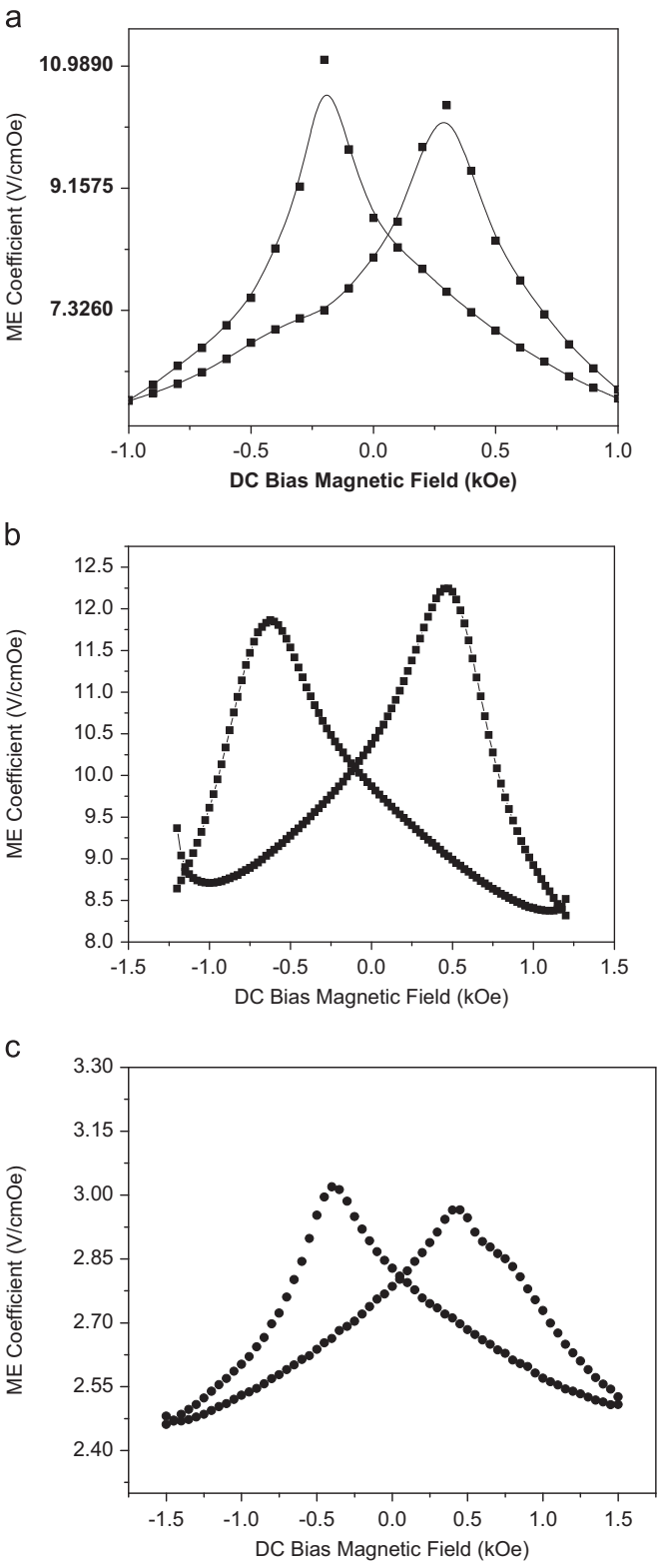

Fig. 6. Magnetoelectric coefficient dependence on dc bias magnetic field of thin films deposited by the polymeric precursor method at 500 °C in static air for 2 h at a 7 kHz ac magnetic field at room temperature (a) BFO; (b) BLF and (c) BNF.

ferromagnetism. The appearance of weak ferromagnetism in this compound may be attributed to either the canting of the antiferromagnetically ordered spins by a structural distortion [53–55] or the breakdown of the balance between the antiparallel sublattice magnetization of Fe^{3+} due to metal ion substitution with a different valence [56]. The magnetization linearly increases with the applied magnetic field which is characteristic of antiferromagnets and Nd and La ions change the pure bismuth ferrite magnetic structure. A change in the magnetic properties in this case is explained not only by different magnetic moments and ion radii of neodymium and lanthanum (the La and Nd atoms do not possess any intrinsic magnetic moment), but also by the anisotropy of the magnetic moments of La and Nd ions. The magnetization appears enhanced due to magnetic ordering on La and Nd substitution. This enhancement may be attributed to different factors like (i) structural distortion due to La and Nd substitution, (ii) variation in the oxygen stoichiometry or Fe^{2+} ion, (iii) reduction in grain size and (iv) change in the magnetic anisotropy, etc [57,58]. Further studies are required to understand the magnetic behavior of this compound. The low coercive magnetic fields of rare-earth substituted BFO films are indicative of their magnetically soft nature which makes these films suitable for device applications.

The magnetolectric coefficient versus dc bias magnetic field in the longitudinal direction reveals hysteretic behavior, as observed in the magnetic field cycles shown in Fig. 6. The magnetoelectric coefficient of BLF and BNF are 10 V/cm Oe and 12 V/cm Oe respectively which are much larger than that previously reported for thin films as high as 3 V/cm Oe in the same direction at zero fields [59] (Fig. 6b–c). This is a consequence of the antiferromagnetic axis of BLF and BNF which rotates through the crystal with an incommensurate long-wavelength period of ~620 Å [60,61]. Early reports showed that the spiral spin structure leads to a cancellation of any macroscopic magnetization and would inhibit the observation of the linear magnetoelectric effect [62]. Significant magnetization (~0.5 μB/unitcell) and a strong magnetoelectric coupling have been observed in epitaxial thin films, suggesting that the spiral spin structure could be suppressed [63].

The domain structures observed in the film by piezoelectric force microscopy (PFM) was illustrated in Fig. 7. The out-of-plane (OP) and in-plane (IP) piezoresponse images of the as-grown films after applying a bias of −12 V, on an area of 2 μm × 2 μm, and then an opposite bias of +12 V in the central 1 μm × 1 μm area were employed. To obtain the domain images of the films, a high voltage that exceeds the coercive field was applied during scanning. The contrast in these images is associated with the direction of the polarization [64]. The PFM image indicates that the perpendicular component of polarization can be switched between two stable states: bright and dark contrast inside and outside of the square region. Higher PFM magnification images showed that the regions without piezoresponse exhibit a strong contrast in the PFM images. The white regions in the out-of-plane PFM images correspond to domains with the polarization vector oriented toward the bottom electrode hereafter referred to as down polarization (Fig. 7a), while the dark regions correspond to domains oriented upward referred to as up polarization. Grains which exhibit no contrast change is associated with zero out-of-plane polarization. A similar situation was observed when a positive bias was applied to the film. We noticed that some of the grains exhibit a white contrast associated to a component of the polarization pointing toward the bottom electrode. On the other hand, in the in-plane PFM images (Fig. 7b) the contrast changes were associated with changes of the in-plane polarization components. In this case, the white contrast indicates polarization e.g. in the positive direction of the y-axis while dark contrast are given by in-plane polarization components pointing to the negative part of the y-axis. The ferroeletric domains in the BLF and BNF films consist of a multiple domain state in a mixture of 71° and 180° domains which grow large into blocks. The domains grow in multiple states is a consequence of films thickness being close to 300 nm. In this way, rare-earth acts reducing the strain energy and the pinning effect of charged defects. The main differences in the out-of-plane (OP) and in-plane (IP) piezoresponse images may be understood as follows: first, the piezoelectric tensor for the tetragonal symmetry is complex, resulting in an effective piezoelectric coefficient that is not proportional to the component of polarization along the detection direction, as explained in Ref. [65]. In this scenario, the IP response may not change its sign upon polarization switching, while the OP response does. Second, the 180° switching process may take place via two non-180° (i.e., 71° and/or 109°, [66]) switching steps, which also implies switching of only one component of the electrical polarization. The piezoelectric response of rare-earth substituted BFO films was higher than that of nonsubstituted BFO film, indicating that the piezoelectricity of the BFO film was improved by the ion modification using rare-earth cations. We recognize that the rare-earth substitution for BFO film would result in changes on crystal anisotropy and piezoelectricity, as well as improvement of the insulating property reported in the previous research [67]. The lattice volume of perovskite based crystals decreased by A-site substitution using rare earth cations, which is based on the relaxation of the structural distortion of an iron octahedral environment and the O–Fe–O and Fe–O–Fe angles, as similar to BIT crystal [68]. Also, the spontaneous polarization of BFO crystal could be enhanced if the polar axis could be elongated based on the ion modification, as discussed in the studies of PZT films [69].

The d_{33} (V) hysteresis loop is shown in Fig. 8. The hysteresis in the piezoresponse signal is directly associated with the polarization switching and ferroelectric properties of the film. The maximum d_{33} value, ~80 pm/V for the BNF film is better than the reported value for a BFO deposited on Si [70] and approaches the reported value for

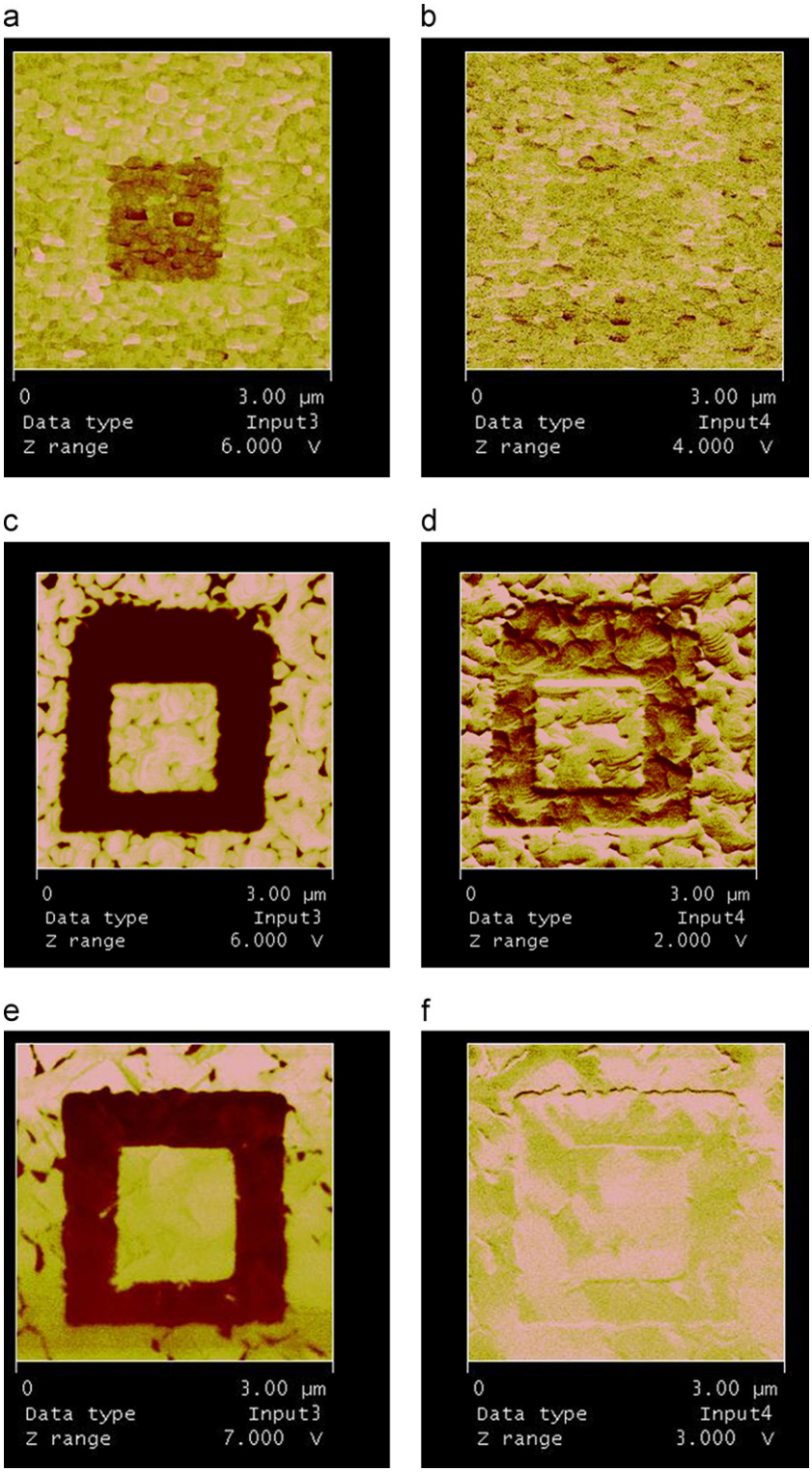

Fig. 7. Out-of-plane (OP) and in-plane (IP) PFM images of thin films deposited by the polymeric precursor method at 500 °C in static air for 2 h (a) BFO (OP); (b) BFO (IP); (c) BLF (OP); (d) BLF (IP); (e) BNF(OP) and (f) BNF (IP).

a BIT single crystal [71]. The enhancement of polarization could be caused by the relaxation of the structural distortion of an iron octahedral environment and the O–Fe–O and Fe–O–Fe angles which reduces the initial nucleation rate when crystallizing the film. The presented value reported for our BNF film suggests that this material can be considered as a viable alternative for lead-free piezo-ferroelectric devices. Here, we point out that it is difficult to compare these values to the piezoelectric coefficients of bulk material since the measurement was performed on a local area that has a relatively intricate field distribution and vibrational modes. Considering the

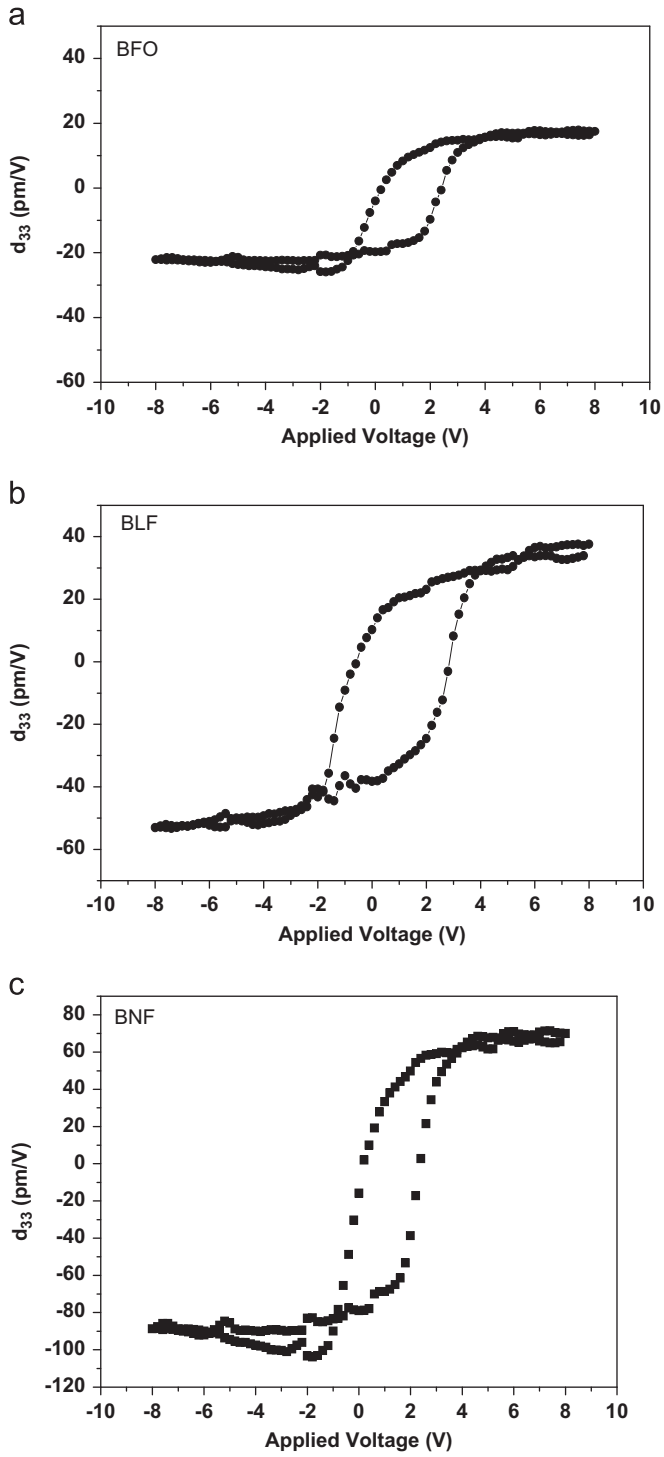

Fig. 8. Piezoelectric coefficient loop, $d_{33,}$ of thin films deposited by the polymeric precursor method at 500 °C in static air for 2 h (a) BFO; (b) BLF and (c) BNF.

polycrystalline nature of our films the effective piezoelectric coefficient depends on grain orientation. Therefore, as expected the piezoelectric response increases with rare-earth addition due to the change in crystal structure and reduction in the strain energy and the pinning effect of charged defects after doping. Although the PZT films still have higher d_{33} values, ranging from 40 to 110 pm/V [72], the presented values reported for our BNF films suggest that this material can be considered as a viable alternative for lead-free piezo-ferroelectric devices. In comparison with other lead free ferroelectrics, 80 pm/V is much higher than the d_{33} value of Nd-doped $Bi_4Ti_3O_{12}$ [73] (38 pm/V).

4. Conclusions

Rare-earth-substituted BFO films were fabricated using a soft chemical method technique to investigate the influence of ion modification using rare-earth cations on crystal structure, as well as insulating and magnetic properties of BFO thin films. A tetragonal BFO crystalline phase was obtained on Pt (111)/Ti/SiO_2/Si substrates by heat treatment in ambient conditions at 500 °C for 2 h. Ion modification using La^{3+} and Nd^{3+} cations suppressed the leakage current conduction of BFO film at room temperature. Nd substitution plays an important role not only improving electrical properties of BFO films but also improving magnetic properties. The maximum magnetoelectric coefficient was close to 12 V/cm Oe for the BNF film in the longitudinal direction. It was found that 71° and 180° domain switchings, and pinned domain formation can occur in BLF and BNF thin films. La and Nd substitution was found to effectively induce spontaneous magnetization in antiferromagnetic $BiFeO_3$ exhibiting good piezoelectric properties. This material should provide useful guidelines for preparing BFO-based materials with controlled properties for low-power-consumption micro transducers in piezoelectric-based MEMS applications.

Acknowledgments

The financial support of this research project by the Brazilian research funding agencies CNPq and FAPESP is gratefully acknowledged.

References

[1] G.D. Achenbach, W.J. James, R. Gerson, Preparation of single-phase polycrystalline $BiFeO_3$, Journal of the American Chemistry Society 50 (8) (1967) 437.
[2] C. Michel, J.M. Moreau, G.D. Achenbach, R. Gerson, W.J. James, Atomic structure of bismuth(III) ferrate(III), Solid State Communications 7 (9) (1969) 701–704.
[3] A.J. Jacobson, B.E.F. Fender, Neutron diffraction study of the nuclear and magnetic structure of bismuth iron trioxide, Journal of Physics C 8 (6) (1975) 844–850.
[4] M. Polomska, W. Kaczmarek, Z. Pajak, Electric and magnetic properties of bismuth lanthanum iron oxide($(B_{1-x}La_x)FeO_3$) solid solutions, Physics Status Solidi A 23 (2) (1974) 567–574.
[5] W. Kaczmarek, Z. Pajak, M. Polomska, Differential thermal analysis of phase transitions in (bismuth, lanthanum) iron oxide $(Bi_{1-x}La_x)FeO_3$ solid solution, Solid State Communications 17 (7) (1975) 807–810.
[6] T.Y. Kim, H.M. Jang, S.M. Cho, Effects of La doping on the cubic-tetragonal phase transition and short-range ordering in $PbTiO_3$, Journal of Applied Physics 91 (1) (2002) 336–343.
[7] L. Carlsson, Crystal structure changes in $BaTiO_3$, Acta Crystallography 20 (3) (1966) 459.

[8] Y.S. Touloukian, R.K. Kirby, R.E. Taylor, T.Y.R. Lee, Thermophysical Properties of Matter; Thermal Expansion—Nonmetallic Solids, IFI/Plenum, New York, 1977, p. 564.
[9] S.A. Mansour, R.W. Vest, The dependence of ferroelectric and fatigue behaviors of PZT films on microstructure and orientation, Integrated Ferroelectrics 1 (1) (1992) 57–69.
[10] J.R. Teague, R. Gerson, W.J. James, Dielectric hysteresis in single crystal bismuth iron (II) oxide, Solid State Communications 8 (13) (1970) 1073–1074.
[11] J.B. Neaton, C. Ederer, U.V. Waghmare, N.A. Spaldin, K.M. Rabe, First-principles study of spontaneous polarization in multiferroic $BiFeO_3$, Physical Review B 71 (1) (2005) 014113/1–014113/8.
[12] J. Wang, J.B. Neaton, H. Zheng, V. Nagarajan, S.B. Ogale, B. Liu, D. Viehland, V. Vaithyanathan, D.G. Schlom, U.V. Waghmare, N.A. Spaldin, K.M. Rabe, M. Wuttig, R. Ramesh, Epitaxial $BiFeO_3$ multiferroic thin-film heterostructures, Science 299 (5613) (2003) 1719–1722.
[13] K.Y. Yun, D. Ricinschi, T. Kanashima, M. Noda, M. Okuyama, Giant ferroelectric polarization beyond 150 $\mu C/cm^2$ in $BiFeO_3$ thin film. Part 2, Japanese Journal of Applied Physics 43 (5A) (2004) L647–L648.
[14] G. Teowee, K. McCarthy, F. McCarthy, T.J. Bukowski, T.P. Alexander, D.R. Uhlmann, Dielectric and ferroelectric properties of sol–gel derived $BiFeO_3$ films, Integrated Ferroelectrics 18 (1–4) (1997) 329–337.
[15] K.Y. Yun, M. Noda, M. Okuyama, Effects of annealing atmosphere on crystallization and electrical properties in $BiFeO_3$ thin films by chemical solution deposition (CSD), Journal of the Korean Physics Society 42 (Suppl. Issue, Proceedings of the 4th Japan–Korea Conference of Ferroelectrics, 2002) (2003) S1153–S1156.
[16] H. Uchida, H. Yoshikawa, I. Okada, H. Matsuda, T. Iijima, T. Watanabe, T. Kojima, H. Funakubo, Approach for enhanced polarization of polycrystalline bismuth titanate films by Nd^{3+}/V^{5+} cosubstitution, Applied Physics Letters 81 (12) (2002) 2229–2231.
[17] W. Eerenstein, F.D. Morrison, J. Dho, M.G. Blamire, J.F. Scott, N.D. Mathur, Comment on Epitaxial $BiFeO_3$ multiferroic thin film heterostructures, Science 307 (5713) (2005) 1203.
[18] H. Béa, M. Bibes, A. Barthelemy, K. Bouzehouane, E. Jacquet, A. Khodan, J.-P. Contour, S. Fusil, F. Wyczisk, A. Forget, Influence of parasitic phases on the properties of $BiFeO_3$ epitaxial thin films, Applied Physics Letters 87 (7) (2005) 072508/1–072508/3.
[19] H. Uchida, I.,.H. Yoshikawa, I. Okada, H. Matsuda, T. Iijima, T. Watanabe, H. Funakubo, J. Jpn, Fabrication of M^{3+}-substituted and M^{3+}/V^{5+}-cosubstituted bismuth titanate thin films [M=lanthanoid] by chemical solution deposition technique. Part 1, Japanese Journal of Applied Physics 41 (11B) (2002) 6820–6824.
[20] H. Nakaki, H. Uchida, S. Okamoto, S. Yokoyama, H. Funakubo, S. Koda, Improvement of ferroelectric properties of lead zirconate titanate thin films by ion-substitution using rare-earth cations, Materials Research Society Symposium Processing 830 (2005) 141–146.
[21] Y. Noguchi, M. Miyayama, Large remanent polarization of vanadium-doped $Bi_4Ti_3O_{12}$, Applied Physics Letters 78 (13) (2001) 1903–1905.
[22] D. Wu, A. Li, T. Zhu, Z. Li, Z. Liu, N. Ming, Processing- and composition-dependent characteristics of chemical solution deposited $Bi_{4-x}La_xTi_3O_{12}$ thin films, Journal of Materials Research 16 (5) (2001) 1325–1332.
[23] W. Sakamoto, M. Yamada, N. Iizawa, Y. Mizutani, D. Togawa, K. Kikuta, T. Yogo, T. Hayashi, S. Hirano, Preparation and properties of $Bi_{4-x}Nd_xTi_3O_{12}$ thin films by chemical solution deposition, Journal of Electroceramics 13 (1/2/3) (2004) 339–343.
[24] T. Goto, Y. Noguchi, M. Soga, M. Miyayama, Effects of Nd substitution on the polarization properties and electronic structures of bismuth titanate single crystals, Materials Research Bulletin 40 (6) (2005) 1044–1051.
[25] K. Tominaga, A. Shirayanagi, T. Takagi, M. Okada, Switching and fatigue characteristics of lead lanthanum zirconate titanate thin films by metalorganic chemical vapor deposition. Part 1, Japanese Journal of Applied Physics 32 (9B) (1993) 4082–4085.
[26] J.W. Hyun, G.B. Kim, Electric properties of La-modified lead titanate thin films fabricated by sol–gel processing, Journal of Korean Physics Society 42 (1) (2003) 139–142.
[27] M. Shimizu, H. Fujisawa, T. Shiosaki, MOCVD of ferroelectric PLZT thin films and their properties, Microelectronic Engnineering 29 (1-4) (1995) 173–176.
[28] Z.V. Gabbasova, M.D. Kuz'min, A.K. Zvezdin, I.S. Dubenko, V.A. Murashov, D.N. Ravok, I.B. Krynetskii, Bismuth rare earth(R) iron oxide ($Bi_{1-x}R_xFeO_3$): a family of novel magnetoelectrics, Physical Letters A 158 (9) (1991) 491–498.
[29] V.A. Murashov, D.N. Rakov, V.M. Ionov, I.S. Dubeko, Y.V. Titov, V.S. Gorelik, Magnetoelectric (Bi, Ln)FeO_3 compounds: crystal growth, structure, and properties, Ferroelectrics 162 (1–4) (1994) 359–369.
[30] A.M. Kadomtseva, Y.F. Popov, T.V. Schogoleva, G.P. Vorob'ev, A.K. Zvezdin, I.S. Dubenko, V.A. Murashov, D.N. Rakov, High magnetic field investigations of the magnetoelectric effect in magnetic ferroelectrics (RBi)FeO_3, Ferroelectrics 169 (1–4) (1995) 85–95.
[31] H. Uchida, R. Ueno, H. Nakaki, H. Funakubo, S. Koda, Ion modification for improvement of insulating and ferroelectric properties of $BiFeO_3$ thin films fabricated by chemical solution deposition, Japanese Journal of Applied Physics 44 (2) (2005) L561–L564.
[32] R.D. Shannon, Revised effective ionic radii and systematic studies of interatomic distances in halides and chalcogenides, Acta Crystallogaphica Section A: Crystal Physics, Diffraction, Theoretical and General Crystallography 32 (5) (1976) 751–767.
[33] H. Uchida, H. Yoshikawa, I. Okada, H. Matsuda, T. Iijima, T. Watanabe, T. Kojima, H. Funakubo, Approach for enhanced polarization of polycrystalline bismuth titanate films by Nd^{3+}/V^{5+} cosubstitution, Applied Physics Letters 81 (12) (2001) 2229–2231.
[34] A.Z. Simoes, A.H.M. Gonzalez, C.S. Riccardi, E.C. Souza, F. Moura, M.A. Zaghete, E. Longo, J.A. Varela., Ferroelectric and dielectric properties of lanthanum modified bismuth titanate thin films obtained by the polymeric precursor method, Journal of Electroceramics 13 (1-3) (2004) 65–70.
[35] A.Z. Simões, B.D. Stojanovic, M.A. Zaghete, C.S. Riccardi, A. Ries, F. Moura, E. Longo, J.A. Varela, Electrical characterization of lanthanum-modified bismuth titanate thin films obtained by the polymeric precursor method, Integrated Ferroelectrics 60 (2004) 21–31.
[36] A.Z. Simões, C.S. Riccardi, L.S. Cavalcante, J.A. Varela, E. Longo, Size effects of polycrystalline lanthanum modified $Bi_4Ti_3O_{12}$ thin films, Materials Research Bulletin 43 (1) (2008) 158–167.
[37] A.Z. Simões, L.S. Cavalcante, C.S. Riccardi, J.A. Varela, E. Longo, Ferroelectric and dielectric behaviour of $Bi_{0.92}La_{0.08}FeO_3$ multiferroic thin films prepared by soft chemistry route, Journal of Sol–Gel Science and Technology 3 (1) (2007) 269–273.
[38] A.H.M. Gonzalez, A.Z. Simões, L.S. Cavalcante, E. Longo, J.A. Varela, C.S. Riccardi, Retention characteristics in $Bi_{3.25}La_{0.75}Ti_3O_{12}$ thin films prepared by the polymeric precursor method, Applied Physics Letters 86 (11) (2005) 11911–112909.
[39] A.Z. Simões, C.S. Riccardi, L.S. Cavalcante, E. Longo, J.A. Varela, B. Mizaikoff, D. Hess, Ferroelectric characteristics of $BiFeO_3$ thin films prepared via a simple chemical solution deposition, Journal of Applied Physics 101 (7) (2007) 074108–074112.
[40] A.Z. Simões, M.A. Ramirez, C.S. Riccardi, E. Longo, J.A. Varela., Ferroelectric characteristics of $SrBi_4Ti_4O_{15}$ thin films grow on Pt/Ti/SiO_2/Si substrates by the soft chemical method, Materials Letters 60 (16) (2006) 2020–2023.
[41] A.Z. Simões, M.A. Ramirez, N.A. Perucci, C.S. Riccardi, E. Longo, J.A. Varela., Retention characteristics in $Bi_{3.25}La_{0.75}Ti_3O_{12}$ thin films prepared by the polymeric precursor method, Applied Physics Letters 86 (11) (2005) 112909.
[42] W. Eerenstein, F.D. Morrison, J. Dho, M.G. Blamire, J.F. Scott, N.D. Mathur, Multiferroic and magnetoelectric materials, Nature 442 (17) (2006) 759–765.

[43] H. Béa, M. Bibes, A. Barthelemy, K. Bouzehouane, E. Jacquet, A. Khodan, J.-P. Contour, S. Fusil, F. Wyczisk, A. Forget, Influence of parasitic phases on the properties of $BiFeO_3$ epitaxial thin films, Applied Physics Letters 87 (7) (2005) 072508/1–072508/3.

[44] H. Uchida, I. Okada, H. Matsuda, T. Iijima, T. Watanabe, H. Funakubo, Fabrication of M^{3+}-substituted and M^{3+}/V^{5+}-cosubstituted bismuth titanate thin films [M = lanthanoid] by chemical solution deposition technique, Japanese Journal of Applied Physics 41 (1) (2002) 6820–6823.

[45] H. Nakaki, H. Uchida, S. Okamoto, S. Yokoyama, H. Funakubo, S. Koda, Improvement of ferroelectric properties of lead zirconate titanate thin films by ion-substitution using rare-earth cations, Materials Research Society Symposium Processing 830 (2005) 141–146.

[46] Y. Noguchi, M. Miyayama, Large remanent polarization of vanadium-doped $Bi_4Ti_3O_{12}$, Applied Physics Letters 78 (13) (2001) 1903–1905.

[47] D. Wu, A. Li, T. Zhu, Z. Li, Z. Liu, N. Ming, Processing-and composition-dependent characteristics of chemical solution deposited $Bi_{4-x}La_xTi_3O_{12}$ thin films, Journal Materials Research 16 (5) (2001) 1325–1332.

[48] W. Sakamoto, T. Yogo, Synthesis and properties of ferroelectric Si-doped (Bi, Nd)$_4Ti_3O_{12}$ thin films by chemical solution deposition, Journal of Electroceramics 17 (2) (2006) 293–297.

[49] T. Goto, Y. Noguchi, M. Soga, M. Miyayama, Effects of Nd substitution on the polarization properties and electronic structures of bismuth titanate single crystals, Materials Research Bulletin 40 (2) (2005) 1044–1051.

[50] K. Tominaga, A. Shirayanagi, T. Takagi, M. Okada, Switching and fatigue characteristics of (Pb, La)(Zr, Ti)O_3 Thin films by metalorganic chemical vapor deposition, Japanese Journal of Applied Physics 32 (1) (1993) 4082–4085.

[51] G.A. Gehring, On the microscopic theory of the magnetoelectric effect, Ferroelectrics 161 (1) (1994) 275–285.

[52] J.B. Goodenough and J.M. Lango Landolt-Bornstein numerical data and functional relationships in science and technology vol. III/4a (New York: Springer, (1978).

[53] Y.P. Wang, L. Zhou, M.F. Zhang, X.Y. Chen, J.M. Liu, Z.G. Liu, Room-temperature saturated ferroelectric polarization in $BiFeO_3$ ceramics synthesized by rapid liquid phase sintering, Applied Physics Letters 84 (1) (2004) 1731–1734.

[54] V.R. Palkar, R. Pinto, $BiFeO_3$ thin films: novel effects, Pramana 58 (5,6) (2002) 1003–1008.

[55] H. Nakaki, H. Uchida, K. Nishida, M. Osada, H. Funakubo, T. Katoda, S. Koda, Structural and dielectric properties of Ga-modified $BiFeO_3$–$PbTiO_3$ crystalline solutions, Japanese Journal of the Applied Physics 44 (1) (2005) 6905–6908.

[56] H. Uchida, R. Ueno, H. Nakaki, H. Funakubo, S. Koda, Ion modification for improvement of insulating and ferroelectric properties of $BiFeO_3$ thin films fabricated by chemical solution deposition, Japanese Journal of the Applied Physics Part 2 44 (16–19) (2005) L561–L563.

[57] G.A. Smolenskii, V.M. Yudin, Antiferromagnetic properties of some perovskite, Soviet Physics JETP 16 (1963) 622–624.

[58] K. Lukaszewicz, J. Karut-Kalicinska, X-ray investigations of the crystal structure and phase transitions of $YMnO_3$, Ferroelectrics 7 (236) (1974) 81–82.

[59] A.F. Devonshire, Theory of barium titanate. I, Philosofical Magazine 40 (1949) 1040–1063.

[60] M.J. Haun, E. Furman, S.J. Jang, H.A. McKinstry, L.E. Cross, Modeling of the electrostrictive, dielectric and piezoelectric properties of ceramic $PbTiO_3$, Journal of Applied Physics 62 (2) (1987) 3331–3335.

[61] V.A. Murashov, D.N. Rakov, V.M. Ionov, I.S. Dubenko, Y.V. Titov, V.S. Gorelik, Magnetoelectric (Bi, Ln)FeO_3 compounds: crystal growth, structure and properties, Ferroelectrics 162 (135) (1994) 11–21.

[62] I. Sosnowska, R. Przenioslo, P. Fischer, V.A. Murashov, Neutron diffraction studies of the crystal and magnetic structures of $BiFeO_3$ and $Bi_{0.93}La_{0.07}FeO_3$, Journal of Magnetic Material 160 (1) (1996) 384.

[63] Y. Shimakawa, Y. Kubo, Y. Tauchi, H. Asano, T. Kamiyama, F. Izumi, Z. Hiroi, Crystal and electronic structures of $Bi_{4-x}La_x$-Ti_3O_{12} ferroelectric materials, Applied Physics Letters 79 (17) (2001) 2791–2793.

[64] H. Nakaki, H. Uchida, S. Yokoyama, H. Funakubo, S. Koda, Enhancement of spontaneous polarization in lead zirconate titanate thin films by Dy^{3+} substitution, Japanese Journal of Applied Physics 43 (1) (2004) 6551–6558.

[65] H. Nakaki, H. Uchida, S. Koda, S. Okamoto, H. Funakubo, K. Nishida, T. Katoda, K. Saito, Enhancement of spontaneous polarization in lead zirconate titanate thin films by Dy^{3+} substitution, Applied Physics Letters 87 (18) (2005) 182906/1–182906/3.

[66] J.R. Chen, N. Li, L.E. Cross, Structural and dielectric properties of Ga-modified $BiFeO_3$–$PbTiO_3$ crystalline solutions, Journal of Applied Physics 94 (8) (2005) 5153–5157.

[67] F.M. Pontes, E.R. Leite, E. Longo, J.A. Varela, E.B. Araujo, J.A. Eiras, Photoluminescence at room temperature in amorphous $SrTiO_3$ thin films obtained by chemical solution deposition, Applied Physics Letters 76 (2) (2000) 2433–2435.

[68] M.M. Kumar, S. Srinath, G.S. Kumar, S.V. Suryanarayana, Spontaneous magnetic moment in $BiFeO_3$–$BaTiO_3$ solid solutions at low temperatures, Journal of Magnetic Material 188 (1) (1998) 203–212.

[69] T. Kanai, S.I. Ohkoshi, A. Nakajima, T. Watanabe, K. Hashimoto, Magnetic, electric, and optical functionalities of $(PLZT)_x(BiFeO_3)_{1-x}$ ferroelectric–ferromagnetic thin films, Journal of Physical Chemistry Solids 64 (3) (2003) 391–397.

[70] J. Wang, J.B. Neaton, H. Zheng, V. Nagarajan, S.B. Ogale, B. Liu, D. Viehland, V. Vaithyanathan, D.G. Schlom, U.V. Waghmare, N.A. Spaldin, K.M. Rabe, M. Wuttig, R. Ramesh, Epitaxial $BiFeO_3$ multiferroic thin film heterostructures, Science 299 (24) (2003) 1719–1722.

[71] K. Ueda, H. Tabata, T. Kawai, Coexistence of ferroelectricity and ferromagnetism in $BiFeO_3$–$BaTiO_3$ thin films at room temperature, Applied Physics Letters 75 (4) (1999) 555–557.

[72] Q.H. Jiang, C.W. Nanw, Z.J. Shen, Synthesis and properties of multiferroic La-modified $BiFeO_3$ ceramics, Journal of the American Ceramics Society 89 (7) (2006) 2123–2127.

[73] S.T. Zhang, M.H. Lu, D. Wu, Y.F. Chen, N.B. Ming, Larger polarization and weak ferromagnetism in quenched $BiFeO_3$ ceramics with a distorted rhombohedral crystal structure, Applied Physics Letters 87 (26) (2005) 262907/1–262907/3.